Bulletin of the Faculty of Engineering, Assiut University, Vol. 28, No. 2, May 2000.

ANALYSIS OF A PROPAGATING GAUSSIAN LIGHT BEAM INCIDENT AT THE CRITICAL ANGLE ON A DIELECTRIC INTERFACE BY THE BPM

Lotfi Rabeh Gomaa *

(Received November, 15, 1999 Accepted February, 13, 2000)

ملخص: – طريقة الشعاع المنتشر استخدمت فى دراسة خصائص شعاع ضوئى وحيد اللون من نوع جاوس ساقط بالزاوية الحرجة على سطح فاصل بين وسطين عازلين. الخصائص الأساسية للانعكاس التام للأشعة المحدودة فراغيا درست باستفاضة و نوقشت. بعض الظواهر التي لم يسبق دراستها تمت مناقشتها مثل: الموجات الموقوفة الناتجة عن تداخل الأشعة الساقطة و المنعكسة، كذلك الأتساع الفراغى للشعاع المنكسر فى الوسط منخفض الكثافة الضوئية و اتجاه انتشاره. كما درس المجال السطحى و ازاحة جوس–هانشن. كما درست الخصائص الخافتة للمجال المضمحل فى الوسط منخفض الكثافة الضوئية. و قد اتفقت نتائج البحث مع نتائج طرق عددية اخرى اكثر تعقيدا.

ABSTRACT *– The characteristics of a gaussian monochromatic light beam incident at the critical angle of incidence on a dielectric interface are investigated using the Beam Propagation Method (BPM). The main features relevant to the total internal reflection of spatially-bounded light beams are thoroughly investigated and discussed. Some previously unexamined phenomena: standing waves resulting from the interference of the incident and reflected beams, as well as the angular spread of the refracted beam in the rarer medium and its direction of propagation are considered. The lateral field and the Goos-Hänchen shift are also investigated and the results obtained by the BPM are in agreement with those obtained by other more involved numerical methods.*

INTRODUCTION

The phenomenon of total reflection of gaussian light beams is of significant importance in the field of integrated optics and fiber-based communication systems, because such beams represent well the dominant mode of a single-mode fiber and laser diodes and oscillators. It is worthy to point out that most of the guidance phenomena rely on total reflection at a dielectric interface, and actually guided fields are spatially-bounded. Despite of this fact, most of the analytical methods used in the analytical methods used in the analysis of guided-wave phenomena assume guided plane waves rather than the more realistic spatially-bounded fields. This reflects the need of simple, powerful and versatile method in the analysis of the guidance phenomena of such fields. There are three main features relevant to the process of total reflection at critical incidence: the lateral displacement (Goos-Hänchen shift) of the reflected and transmitted beams from the position predicted by geometrical optics [1], the penetration of energy in the less dense medium where the field is basically evanescent and the lateral field which extends well beyond the reflected and transmitted fields [1,2]. Pioneering research papers [3-6] were concerned with well collimated beams where the quotient : "beam waist/wavelength" varies from 100 to 10^4. Unfortunately, this condition is not met in the majority of single-mode integrated-optical components and fiber-based communication systems. Nevertheless in Antar's paper [1] the smallest value of the (beam waist/wavelength) was equal to 10 ; which is a quite reasonable value from the practical point of view. The analytical method used by Antar is involved because the

* Faculty of Engineering of Shobra, Zaqaziq University, Banha branch, Egypt.

electromagnetic field is expressed in terms of a complex integral which can be evaluated approximately in terms of an infinite series involving parabolic cylinder functions (each one of them is calculated by an infinite series). Despite of the complexity of Antar's method, no closed form analytic expressions (even approximate) for the Goos-Hänchen shift, or the lateral field, or the refracted field in the rarer medium could be obtained.

An approach based on an angular spectrum representation of the electromagnetic field had been proposed by McGuirck et. al.[7] but it did not lead to any numerical application. Obviously, a simple and powerful analytical method leading to a simple numerical implementation would be of great advantage and benefit.

We believe that the BPM [8,9], is to our knowledge, the most powerful method relying on the angular spectrum representation of the electromagnetic field and has the simplicity and powerfulness we seek at both levels: analytical and numerical. This is justified by the very wide class of problems which had been handled by that method [10-18]: the fundamental characteristics of optical fibers, waveguide modulators and couplers, bent waveguides, nonlinear effects in fibers, solitons and propagation in anisotropic media.

In this paper we present, for the first time to our knowledge, an analysis by the BPM of the phenomenon of total reflection of a gaussian light beam incident on a dielectric interface at the critical angle of incidence because at that angle, the main relevant features [1,2] of the phenomenon of total reflection are strongly manifested: the diffraction effects of the lateral field, the refraction of some energy in the rarer medium and the Goos-Hänchen shift. It is worthy to point out that some analytical and numerical methods are invalid at the critical angle of incidence; so we think that it is a good opportunity to test the validity and the powerfulness of the BPM at that angle of incidence. Because the literature on the BPM is so extensive, a brief review of the method as well as some numerical precautions are presented in an appendix at the end of the paper.

2- FORMULATION OF THE PROBLEM AND THE ESSENCE OF THE BPM

As shown in figure 1, the plane x=0 is the interface between two dielectric media having refractive indices n_1 and n_2 respectively; with $n_1 > n_2$. The geometry of the problem is invariant with respect to the y-coordinate. In the plane y=0 and at $x=x_d$ a monochromatic gaussian light beam at the free-space wavelength λ_o propagates towards the interface.

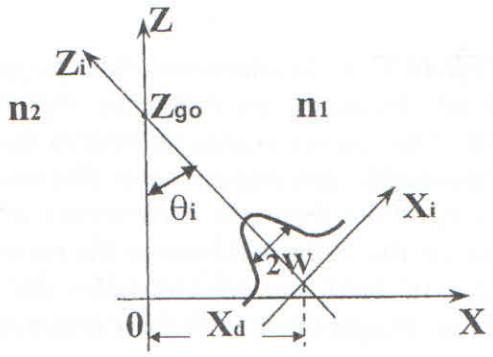

Fig. 1: Gaussian beam incident on a plane dielectric interface.

The beam's axis makes an angle θ_i with respect to the z-axis, this corresponds to the critical angle of incidence $\theta_c = \sin^{-1}(n_1/n_2)$ measured with respect to the normal to the interface. Z_{go} is the point of intersection of the beam's axis with the z-axis. This is the point of total reflection predicted by geometrical optics. The beam width at the waist is 2W (where W is half of the total 1/e width). The time dependence is assumed exp(-iωt), where "i" is the imaginary unity. The electric field of the gaussian beam is y-polarized and hence, in the incident-beam coordinate system (x_i,z_i), can be writen as:

$$E_{yi}(x_i,z_i) = \exp - (x_i/W)^2 \cdot \exp(ik_1 z_i) \qquad (1)$$

Where $k_1 = k_o n_1$ is the wavenumber in the denser medium (i.e. in x>0) and k_o is the free-

space wavenumber. In the interface-coordinate system (x,z) and at z=0, the gaussian distribution in (1) can be written as:

$$E_y(x,0) = \exp -[(x-x_d) \cdot \cos\theta_i / W]^2 \cdot \exp[(ik_1 (x - x_d) \sin\theta_i] \qquad (2)$$

The BPM, first introduced by Fleck et. al.[8], relies on the expansion of $E_y(x,0)$ as a continuous spectrum of plane waves (i.e. a spatial Fourier transform). Each component of the spectrum is made to propagate for a small step Δz in a homogeneous (reference) medium having a refractive index n_o where $n_2 \leq n_o \leq n_1$. Then, Fourier-inverting the propagated spectrum we recover the field at $z = \Delta z$, i.e. $E_y(x, \Delta z)$. Finally, to take into account for the deviation $\delta n(x)$ of the actual refractive index distribution n(x) from the reference value n_o we correct the phase of $E_y(x, \Delta z)$ through multiplication by $\exp[ik_o \delta n(x).\Delta z]$ to obtain the field $E_y(x, \Delta z)$ at $z = \Delta z$. This procedure is summarized as follows:

a- Calculate: $\boldsymbol{F}\{ E_y(x,0) \}$, where "$\boldsymbol{F}$" stands for the Fourier transform operation.

b- Multiply $\boldsymbol{F}\{ E_y(x,0) \}$ by the propagator operator **P**.

c- Calculate $\boldsymbol{F}^{-1}$ (the inverse Fourier transform) of the propagated spectrum obtained in step (b) to recover the uncorrected field $E'_y(x, \Delta z)$.

d- Calculate $\mathbf{Q}\{ E'_y(x, \Delta z) \}$, where **Q** stands for the phase correction operator, to obtain finally $E_y(x, \Delta z)$.

This step-by-step propagation process is continued to any desired distance z. An inherent limitation in the BPM is that any "back-reflected" field (i.e. in the negative z direction) is ignored. Fortunately, in our problem there is no back-reflection from the dielectric interface; only "side-reflection" (i.e. towards the positive x-direction).

3 – WAVE SPECIES AT A DIELECTRIC INTERFACE

The different wave species that can exist at a dielectric interface are best illustrated in figure 2, where three situations are possible:

a- A ray BO incident at an angle less than the critical one, gives rise to a reflected ray OB_r and a refracted ray OB_t obeying Snell's law.

b- A ray AO incident at the critical angle produces a reflected ray OA_r and a lateral ray [1] OA_s which propagates parallel to the interface x=0 and just below it in the less dense medium.

c- A ray CO incident at an angle greater than the critical one giving rise to a totally reflected ray OC_r and a lateral ray OC_s.

The wave species are useful in a qualitative understanding of our problem: a gaussian field can be represented as an angular spectrum of plane waves. Each component in the spectrum corresponds to one of the wave species mentioned above. So, the central component in the spectrum of a beam incident at the critical angle corresponds to the ray AO. For the rest of the components:

1- Half of them are incident at angles less than the critical one; a situation corresponding to rays like OB. These rays contribute to a refracted field in the less dense medium as well as to the reflected field.

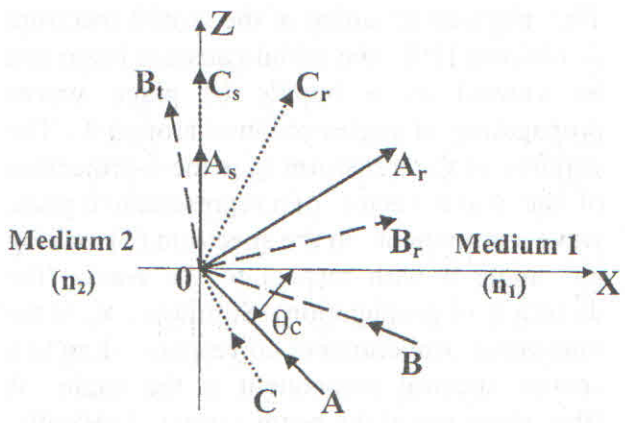

Fig. 2 : Wave species at a plane dielectric interface.

2-The other half are incident at angles greater than the critical one; these correspond to rays like CO, and hence they contribute significantly to the lateral field [1,2] as well as to the reflected field. The lateral field exhibits diffraction effects [1-3] because it extends in the positive z-direction well beyond the point of total reflection Z_{go} predicted by the geometrical optics. Its amplitude is very weak compared to other wave species [1-3] and decreases with z as $(z-z_{go})^{3/2}$, and hence its observation is difficult as pointed out by Antar [1]. Nevertheless, its presence was verified experimentally by many investigators cited in Tamir et.al.[2].

4 - RESULTS AND DISCUSSIONS

For the purpose of comparison, we consider a gaussian beam having the same opto-geometric properties as that one considered by Antar [1] : $W=10\ \lambda_1$, where λ_1 is the wavelength in the denser medium, i.e. $\lambda_1 = \lambda_o/n_1$ and $\lambda_o = 1.55\ \mu m$, $x_d=3W$, $n_1=1.94$ and $n_2=1$. The beam's axis makes an angle θ_i with respect to the z-axis which corresponds to the critical angle of incidence $\theta_c = \sin^{-1}(1/1.94) \approx 31^\circ$, i.e. $\theta_i=(\pi/2) - \theta_c = 59^\circ$. The spatial Fourier spectrum of the initial field (2) is also gaussian [2,3] :

$$E(k_x,0)=(1/\cos\theta_i).\exp-[W(k_x-k_{xi})/2\cos\theta_i]^2.\exp-(i(k_x+k_{xi})x_d] \quad (3)$$

The physical meaning of the spatial spectrum is obvious [19] : the initial gaussian beam can be viewed as a bundle of plane waves propagating at angles centered around θ_i. The variable of the transform k_x is the x-projection of the wave vector of a representative plane wave component in the spectrum (3) making an angle θ with respect to the z-axis (the direction of propagation). Similarly, k_{xi} is the transverse wavenumber correspon- ding to a spatial spectral component at the angle θ_i (the direction of the beam's axis). Evidently, $k_{xi} = k_1 \sin\theta_i = 6.74\ \mu m^{-1}$ and $k_x = k_1 \sin\theta$. From (3), we see that the spectral width, i.e. the total 1/e width of the spatial spectrum of the initial field is $\Delta k_{xi} = 4\cos\theta_i / W = 0.26\ \mu m^{-1}$, and the spectrum is symmetrically centered around the spectral component k_{xi}. Each plane wave component in the spectrum has a z-dependence of the form $\exp(ik_zz)$, where the longitudinal wavenumber k_z follows from the dispersion relation [19] :

$$k_z = (k_1^2 - k_x^2)^{1/2} \quad (4)$$

For $k_x < k_1$, the representative plane wave component is propagating at an angle $\tan^{-1}(k_x/k_z)$ with respect to the z-axis. While for $k_x > k_1$ the representative component is evanescent in the z-direction, i.e. its z-dependence is of the form $\exp(-k_zz)$. Although the evanescent part of the spectrum decays with Z (i.e. it is non propagating), its presence is very important because it describes the fine spatial details of the total propagating field.

Now, we present the results of the calculations and discuss the main features of the total reflection phenomenon:

A - The total propagating field and the standing wave pattern

In figure 3, the total field $E_y(x,z)$ is plotted at different constant-z planes. The total propagated distance is $Z_{tot}= 100\ \mu m$ and the propagation step $\Delta z = 0.1\ \mu m$. The choice of the step size Δz follows from the criterion [9]:

$$|\Delta n_{max}|\ (\Delta z/\lambda_o)\sin^2\theta_{max} << 1 \quad (5)$$

Where Δn_{max} is the maximum deviation of the actual refractive index n(x) from the reference value n_o and θ_{max} is the angle between the direction of the highest significant component in the spatial spectrum of the total propagating field and the z-axis. From (3), a good estimation for the highest significant value of the transverse wavenumber k_x is $k_{x\,max} = k_{xi} + 0.5\,\Delta k_{xi} = 6.87\ \mu m^{-1}$, and hence θ_{max} is equal to $\sin^{-1}(k_{x\,max}/k_1) \approx 61^\circ$, i.e. the total angular spread $\Delta\theta_i$ of the initial gaussian beam around the direction of the beam axis is $2(\theta_{max} - \theta_i) = 4^\circ$.

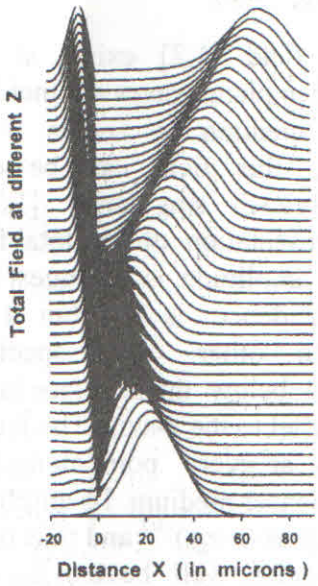

Fig. 3: Total propagating field due to a gaussian beam incident on a dielectric interface at the critical angle.

The dark area (for x>0) shown in figure 3 is the region of interference between the incident and the reflected fields which results in a standing wave pattern.

Figure 4 represents an expanded view of that area; the distance between two successive maxima (or minima) is nearly equal to the expected value $\lambda_1/2 = \lambda_o/2n_1 = 0.4$ μm.

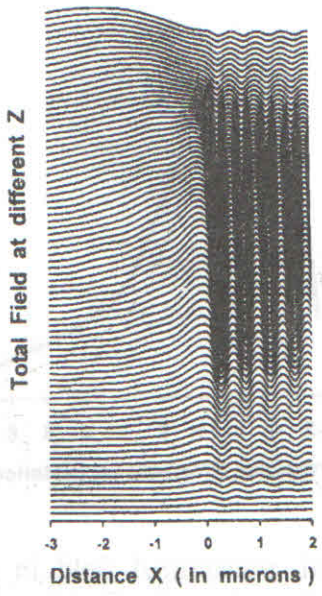

Fig. 4: Standing wave effect in the denser medium n_1 .

B – The transmitted field in the rarer medium and the reflected field

In the region x<0, a peaked field propagates away from the interface x = 0. Figure 5 shows an expanded view of that field which corresponds to the plane wave components in the spectrum of the initial field at angles of incidence less than θ_c and hence they refract in the rarer medium.

To emphasize this result, we refer to figure 6 which represents the spatial spectrum of the total field at the end of the propagation where two peaks are present :

1- The first one pertaining to the transmitted field in the rarer medium occurs at $k_{xt} = 1.23\ \mu m^{-1}$ which corresponds to an angle of refraction in the rarer medium equal to $\theta_t = \sin^{-1}(1.23/k_o n_2) = 17.7^\circ$ with respect to the z-axis, i.e. 72.3° with respect to the normal to the interface. From Snell's law, that angle corresponds to an angle of incidence in the denser medium equal to $\sin^{-1}[(n_2/n_1)\sin 72.3^\circ] = 29.4^\circ < \theta_c$, this explains the refraction in the less dense medium. Assuming that the transmitted field is also gaussian, the highest significant value of the transverse wavenumber in its spectrum corresponding to half its 1/e width is $k_{xt\ max} = 2.1\ \mu m^{-1}$; this corresponds to an angle $\theta_{t\ max} = 31.2^\circ$ with respect to the z-axis, i.e. 58.8° with respect to

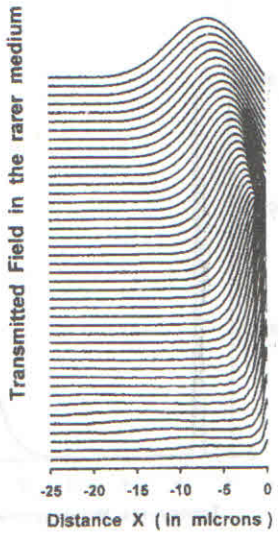

Fig. 5: Total transmitted field in the less dense medium n_2 .

the normal to the interface. The angular spread of the transmitted field in the rarer medium is therefore $\Delta\theta_t = 2(\theta_{t\,max} - \theta_t) = 27^o$, and this corresponds to a spectral width $\Delta k_{xt} = 2(k_{xt\,max} - k_{xt}) = 1.74\ \mu m^{-1}$. If the angular spread per unit spectral width of the initial and transmitted fields are equal, then our assumption on the gaussian shape of the initial field is justified. Direct evaluation of these ratios yields: $(\Delta\theta_i / \Delta k_{xi}) = 15.4$ degree per μm^{-1} and $(\Delta\theta_t / \Delta k_{xt}) = 15.5$ degree per μm^{-1}. The negligible difference between these ratios is due to the fact that the transmitted field is not exactly gaussian as can be seen from figure 6 which shows that the spectrum of that field is not exactly symmetrical around k_{xt}.

2- The second peak in the spectrum shown in figure 6, corresponds to the direction of the reflected beam (with respect to the z-axis). It occurs at $k_x = -6.74\ \mu m^{-1}$, which is numerically equal to the transverse wavenumber corresponding to the direction of the axis of the incident gaussian beam. The negative sign means that the incident and reflected beams propagate in opposite directions with respect to the x-axis (the direction of the transverse wavenumber k_x, which is the variable of the spatial Fourier transform). This verifies the equality of the angle of incidence and reflection.

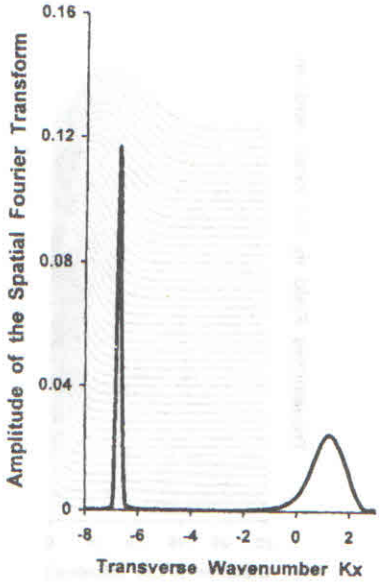

Fig.6: Spatial spectrum of the total field at the end of the propagation distance Z_{tot}.

C- The lateral field

The lateral field [1,2] exists at a plane interface when plane waves are incident from the denser medium at angles $\theta \geq \theta_c$. Analytically, this field can be evaluated through a branch singularity [1,7] in the integral representation of the total field. The lateral field amplitude is strongest when the angle of incidence is θ_c (but it is weak compared to other wave species) and proceeds just below the interface in the rarer medium parallel to the z-axis. The lateral field leaks energy at every point along the z-axis back to the denser medium. Its amplitude fans out gradually as $(z-z_{go})^{-3/2}$ and thus occupies a very wide region well beyond z_{go}. Figure 7 represents a plot of the "total" transmitted field along the interface x=0 as function of of the normalized propagation distance $(z'/w) = (z-z_{go})/w$. The vertical scale is a log-scale, because the very small amplitude of the lateral field contributing to the total field will not be appreciable on a linear scale.

D - The Goos -Hänchen shift

Figure 8 shows the variation of the total field along the interface x = 0 as function of the normalized distance z'/w. The peak of the field is shifted to the right of the point z'=0 by

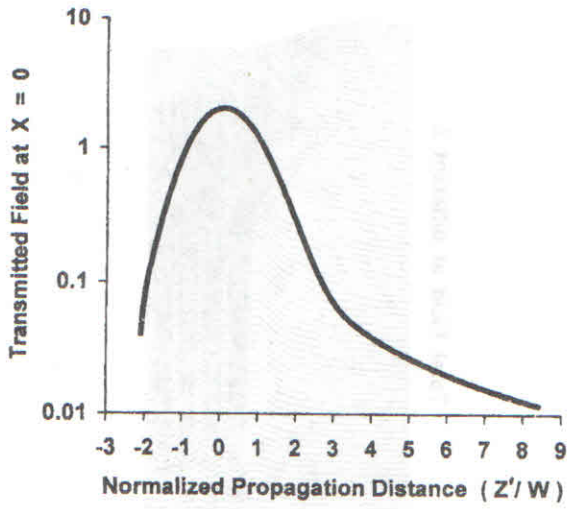

Fig. 7: Total transmitted field in the rarer medium along the interface x = 0, and the behaviour of the lateral field.

an amount equal to 0.244W. Antar [1] found a lateral shift equal to 0.25W; the two values are in good agreement.

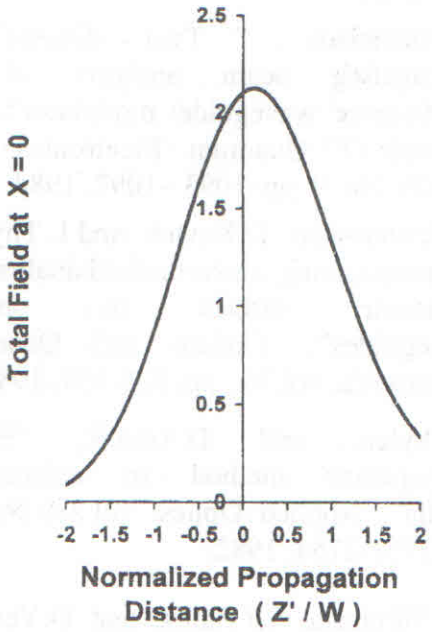

Fig.8: Lateral shift of the total field from the normalized point of incidence Z'/W=0, which corresponds to $Z = Z_{go}$.

E- The evanescent character of the transmitted field

A plot of the peak value of the total transmitted field in the rarer medium as function of the normalized penetration depth x / λ_1 is shown in figure 9. The peak value decreases with increasing x/λ_1. This behavior was pointed out by Antar [1], but no analytical expression governing the evanescence character of the field is available so far. Obviously, there is no reason to expect a simple decay law (for example exponential) of the evanescent field in the rarer medium.

5- CONCLUSIONS

The fundamental characteristics of the total field due to a gaussian beam incident at the critical angle on a dielectric interface are studied using the BPM. It is found that the lateral field varies with Z as $Z^{-3/2}$. The value

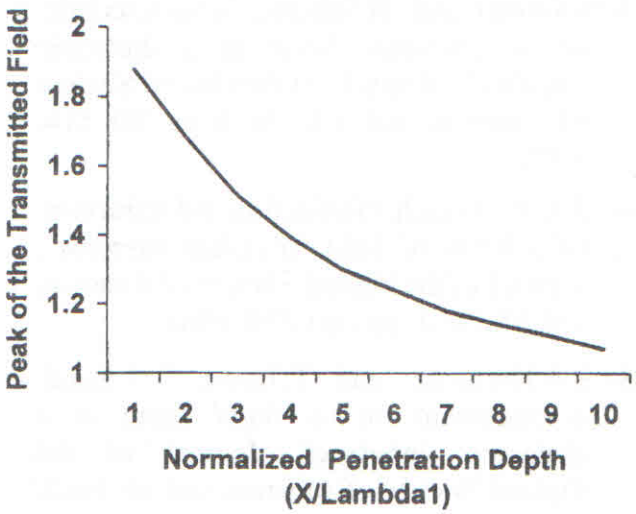

Fig. 9: Evanescent character of the transmitted field in the rarer medium n_2 .

of the Goos-Hänchen shift obtained by the BPM agrees well with that one obtained by other more involved methods. The standing wave character of the total field in the denser medium is examined and the spatial period of the standing wave pattern is verified. An interesting feature is investigated and verified: the transmitted field in the less dense medium comes from that part of the spatial spectrum of the initial propagating field which does not satisfy the condition of total reflection. The peak of the transmitted field is basically evanescent in the direction normal to the interface towards the rarer medium. A noteworthy result is: the shape of the transmitted field is quasi-gaussian and the ratio "angular spread/spectral width" is conserved for both; the initial and transmitted beams.

REFERENCES

1- Y.M.M. Antar, "The transmitted field of a gaussian laser beam at total internal reflections", Canadian Journal of Physics, vol. 55, pp. 2023-2035, 1977.

2- T.Tamir and A.A. Oliner, "Role of the lateral wave in total reflection of light", Journal of the Optical Society of America, vol. 59, No.8, pp. 942-949, 1969.

3- S.Kozaki and H.Sakurai, " Characteristic of a gaussian beam at a dielectric interface", Journal of the Optical Society of America, vol. 68, No.4, pp. 508-514, 1978.

4- H.K.V. Lotsch, "Reflection and refraction of a beam of light at a plane interface", Journal of the Optical Society of America, vol. 58, No.4, pp. 551-556, 1968.

5- B.R.Horowitz and T.Tamir, " Lateral displacement of a light beam at a dielectric interface", Journal of the Optical Society of America, vol. 61, No.5, pp. 586-594, 1969.

6- R.H. Renard, "Total reflection: a new evaluation of the Goos-Hänchen shift", Journal of the Optical Society of America, vol. 54, No.10, pp. 1190-1197, 1964.

7- L.M.Brekhovkikh, "Waves in layered media", Academic Press, New York, 1980.

8- J.A.Fleck, J.R.Morris and M.D.Feit, " Time-dependent propagation of high energy laser beams through the tmosphere", Applied Physics, vol. 10, pp. 129-160, 1976.

9- J.A.Fleck, J..van der Donk and P.E. Lagasse, " Beam - propagation method: analysis and assessment", Journal of the Optical Society of America, vol. 71, No.7, pp. 803- 810, 1981.

10- M.D.Feit and J.A. Fleck, "Mode properties and dispersion for two optical fiber index profiles by the propagating beam method", Applied Optics, vol.19, No.18, pp. 3140-3150, 1980.

11- S.L.Jones, G.Murtaza, J.M. Senior and N.Haigh, " Single – mode optical fiber microbend loss modeling using the finite difference beam propagation method ", Optical Fiber Technology: Materials, Devices and Systems" , vol.4, No.4, pp.471-479, 1998.

12- P.Danielsen and D. Yevick, "Propagating beam analysis of bent optical waveguides", Journal of Optical Communications, vol. 4, No.3, pp. 94-98, 1983.

13- B.Hermansson and D.Yevick, "A propagating beam analysis of optical waveguide couplers", Optical and Quantum Electronics, vol. 16, pp. 131-139, 1984.

14- P. Danielsen , " Two - dimensional propagating beam analysis of an electrooptic waveguide modulator", IEE Journal Of Quantum Electronics, vol. QE-20, No. 9, pp. 1093 –1097, 1984.

15- B.Hermansson, D.Yevick and L.Thylen, "A propagating beam method analysis of nonlinear effects in optical waveguides", Optical and Quantum Electronics, vol.16, pp. 525-534, 1984.

17- L.Thylen and D.Yevick, "Beam propagation method in anisotropic media", Applied Optics, vol.21, No.15, pp. 2751-2754, 1982.

18- J. Sijonmaa, S.J.Halme and D.Yevick, "Beam propagation in elliptic fibers", Optical and Quantum Electronics, vol.14, pp.225-236, 1982.

19- D.Yevick and B.Hermabsson, "Soliton analysis with the propagating beam method", Optics Communications, Vol. 47, pp. 101-106, 1983.

20- J.W.Goodman, "Introduction to Fourier Optics", McGraw-Hill, New York, 1968.

21- E.O.Brigham, "The Fast Fourier Transform", Englewood Cliffs, NJ, Prentice Hall, 1974.

22- D.Storer, "Operator methods in Physical optics", Journal of the Optical Society of America, vol. 71, No. 3, pp. 334-341, 1981.

APPENDIX

The problem under consideration is invariant with respect to the y-coordinate, consequently $\partial^2 / \partial y^2 = 0$ and hence the scalar wave equation for E_y takes the form :

$$[\partial^2 / \partial x^2 + \partial^2 / \partial z^2 + k_o^2 n^2(x)] E_y = 0 \quad (A1)$$

Where n(x) is the refractive index distribution which is function of the transverse coordinate 'x'. Equation (A1) can be written as:

$$\partial^2 E_y/\partial z^2 = - [\nabla_t^2 + k_o^2 n^2(x)] E_y = 0 \quad (A2)$$

Where ∇_t^2 is the transverse laplacian $\partial^2/\partial x^2$. The coefficient of E_y in the right-hand side of (A2) is an operator which depends only on the transverse coordinate 'x' (transverse to the direction of propagation 'Z') and hence, a formal operator solution [21] of (A2) for the forward propagating field at $z=\Delta z$ in terms of its value at z=0 is :

$$E_y(x, \Delta z) = \{\exp (i \Delta z . \mathbf{R})\} . E_y(x,0) \quad (A3)$$

Where a time dependence $\exp(-i\omega t)$ is assumed and **R** is the operator:

$$\mathbf{R} = [\nabla_t^2 + k_o^2 n^2 (x)]^{1/2} \quad (A4)$$

If n(x) is denoted shortly by 'n', then the operator **R** can be written as:

$$\mathbf{R}= [\nabla_t^2 + k_o^2 n^2]^{1/2}$$
$$=\{\nabla_t^2/ [(\nabla_t^2 +k_o^2 n^2)^{1/2} + k_o n]\} + k_o n \quad (A5)$$

If 'n' in the denominator of the first term in the right-hand side of (A5) is replaced by a certain reference value n_o where $n_2 \le n_o \le n_1$ then the last equation can be written as:

$$[\nabla_t^2 + k_o^2 n^2]^{1/2} \approx \{\nabla_t^2/ [(\nabla_t^2 + k^2)^{1/2} + k]\}$$
$$+k +k [(n / n_o) -1] \quad (A6)$$

Where $k=k_o n_o$. The approximation in (A6) is valid if the maximum deviation $\Delta n_{max}(x)$ of n(x) from the reference value n_o satisfies the following criterion [9]:

$$| \Delta n_{max} | (\Delta z / \lambda_o) \sin^2 \theta_{max} << 1 \quad (A7)$$

Where θ_{max} is the angle between the direction of the highest significant plane wave component in the spatial spectrum of the total propagating field and the z-axis. If $E_y(x,z)$ is written as:

$$E_y(x,z) = e_y(x,z) . \exp(ikz) \quad (A8)$$

Then, apart from a constant phase factor $\exp(ik\Delta z)$, direct substitution from (A8) into (A3) gives:

$$e_y(x, \Delta z)=\{\exp[i\Delta z (\mathbf{S}+k_o \delta n)]\}.e_y(x,0) \quad (A9)$$

Where $\delta n = n(x) - n_o$ and $e_y(x,0)$ is the initial field distribution at z=0 (given by eq.(2)). The operator **S** is defined as:

$$\mathbf{S} = \nabla_t^2/ [(\nabla_t^2 + k^2)^{1/2} + k] \quad (A10)$$

The exponent in the right-hand side of (A9) is in fact the product of two operators:

$$[\exp (i \Delta z \ \mathbf{S})] . [\exp (i \Delta z \ k_o \delta n)] \quad (A11)$$

These operators do not commute [21], and hence an approximation is indispensable to evaluate the right-hand side of (A9). It can be shown [21] that to second order in Δz, equation (A9) can be written in a symmetric split-operator [21] form as:

$$e_y(x, \Delta z)=\{\mathbf{P.Q.P} \}.e_y(x,0) + O(\Delta z)^3 \quad (A12)$$

Where $O(\Delta z)^3$ is a negligible term of the order of $(\Delta z)^3$ and **P** and **Q** are the two operators:

$$\mathbf{P} = \exp [i (\Delta z /2) \mathbf{S}] \quad (A13)$$

and :

$$\mathbf{Q} = \exp (i\Delta z \ k_o \delta n) \quad (A14)$$

The operation $\{ \mathbf{P} \} . e_y(x,0)$ represents the propagation of the initial field $e_y(x,0)$ for a distance equal to half the step size $\Delta z/2$ in a homogeneous medium having a constant refractive index n_o , i.e. it is equivalent to solving the Helmholtz wave equation :

$$[\partial^2/ \partial x^2 + \partial^2/ \partial z^2 + k^2] E_y = 0 \quad (A15)$$

with $E_y(x,0)$ as an initial condition at z=0. Therefore, advancing $E_y(x,0)$ by repeated application of (A12) allows us to obtain the total propagating field $E_y(x,z)$ at any distance z once the initial field is known. The operation $\{ \mathbf{P} \} . e_y(x,0)$ is easily performed in Fourier space [9] because the spatial Fourier transform of $\{ \mathbf{P} \} . e_y(x,0)$ can be written as [9,19,20]:

$$F\{ \mathbf{P} \cdot e_y(x,0) \} = \Psi(k_x,0) \cdot \exp \{ (i\Delta z/2) \times k_x^2/[(k^2-k_x^2)^{1/2} + k] \} \quad (A16)$$

Where $\Psi(k_x,0)$ is the spatial Fourier transform of the initial field $e_y(x,0)$, i.e.:

$$\Psi(k_x,0) = \int_{-\infty}^{\infty} e_y(x,0) \cdot \exp(-i k_x x)\, dx \quad (A17)$$

Thus, advancing the initial field for a distance equal to half of the propagation step $\Delta z/2$ by performing $\{\mathbf{P}\} \cdot e_y(x,0)$ in Fourier space (via (A16)), then returning back to the ordinary (x,z) plane by Fourier inversion. To take into account for the deviation of the actual refractive index distribution n(x) from the reference value n_o we multiply the propagated field by the correcting operator **Q**, then performing again the propagation process over the other half propagation step $\Delta z/2$. So, repeated application of these processes allows us to calculate the total propagated field at any distance z. The Fourier transform is calculated numerically from the sampled field values at "N" discrete points x_m where m=1,2,.....N, i.e. a '*D*iscrete *F*ourier *T*ransform'' [20] (DFT) which is calculated by the *F*ast *F*ourier *T*ransform algorithm [20] (FFT). Accordingly, the discrete version of (A17) is written as [20]:

$$\Psi(k_m,0) = \sum_{j=-(N/2)+1}^{N/2} e_y(j\,\Delta x,0).\exp(-i\,k_m .j\,\Delta x) \quad (A18)$$

Where the spacing Δx between the sampled values of the field is calculated from :

$$\Delta x = L/N \quad (A19)$$

'L' being the length of the computational region along the x-axis. The variable of the DFT (the transverse wavenumber) k_m is given by :

$$k_m = 2\pi m/L \quad (A20)$$

From (A19) and (A20), we can write (A18) as:

$$\Psi(k_m,0) = \sum_{j=-(N/2)+1}^{N/2} e_y(j\,\Delta x,0) .\exp(-i\,2\pi mj/N) \quad (A21)$$

The propagation process between z = 0 and z = Δz can be summarized as follows:

1- Calculate the initial spectrum $\Psi\ (k_m, 0)$ from the sampled values $e_y(j\,\Delta x,0)$ at 'N' discrete points using the FFT algorithm.
2- Propagating the initial spectrum over half the step $\Delta z/2$ in the Fourier domain using (A16).
3- Fourier inverting the propagated spectrum using the inverse FFT algorithm to recover the uncorrected field after a half step.
4- Perform the phase correction by multiplying the uncorrected field by the operator **Q**.
5- Repeating the propagation step over the other half step $\Delta z/2$ as described in 1 and 2 to obtain finally the field at z = Δz.

The previous scheme is repeated until we reach the desired propagation distance Z_{tot}. A crucial question regarding the spatial sampling interval Δx: how to choose it?

From the sampling theory we know that as Δx decreases, the resolution (i.e. the ability to capture the fine details) of the spatial Fourier spectrum increases. Consequently, the high spatial frequencies in the spectrum can be "viewed", i.e. the fine variations of the field are considered. The spectrum of the incident field is centered around $k_{xi} = k_1 \sin\theta_i$, and its maximum significant width is $\Delta k_{xi} = 4 \cos\theta_i/W$, and hence the maximum spectral deviation from k_{xi} is $\pm 2\cos\theta_i/W$. From (A20), the maximum value of the transverse wavenumber k_{xmax} in the DFT corresponds to m=N/2, and from (A19) we have:

$$k_{xmax} = \pi / \Delta x \quad (A22)$$

Taking into account for the maximum deviation of k_x from k_{xi} , an acceptable estimate for the maximum value of the transverse wavenumber is: $k_{xmax} = k_{xi} + (2\cos\theta_i/W)$. From (A22), we deduce :

$$(\pi/\Delta x) = k_{xi} + (2\cos\theta_i/W) \qquad (A23)$$

This means that the sampling interval Δx should not exceed $\pi/[k_{xi} + (2\cos\theta_i/W)]$, otherwise the high spatial frequencies in the spectrum would not be "viewed", i.e. the "fine details" of the field would be lost. Thus an acceptable upper limit on the sampling interval Δx is :

$$\Delta x_{max} \leq \pi/[k_{xi} + (2\cos\theta_i/W)] \qquad (A24)$$

Thus, the actual sampling interval Δx must be less than Δx_{max}, for example 0.5 to 0.25 that value. Finally, it is worthy to point out that the propagating field which reaches the boundary of the computational window of width "L", will be reflected back and appears as a fictitious field reflected from the boundary of that window and cause aliasing [8-10]. To prevent this numerical problem, an "absorber" is placed near the edges of the computational window [8-10,20]. A wide variety of absorbers exist. We used "Hanning" truncation function as an absorber, it is defined as [20]:

$$A(x) = 0.5\{1-\cos[2\pi(x-x_d)/L]\} \qquad (A25)$$